RSC Advances

PAPER

View Article Online
View Journal | View Issue

Cite this: *RSC Adv.*, 2024, **14**, 17557

The synthesis and evaluation of novel ALK inhibitors containing the sulfoxide structure†

Han Yao, Yuanyuan Ren, Feng Wu, Jiadai Liu, Longcai Cao, Ming Yan * and Xingshu Li *

Received 1st March 2024
Accepted 10th May 2024

DOI: 10.1039/d4ra01556h

rsc.li/rsc-advances

With ceritinib as the lead, a series of novel compounds containing the sulfoxide structure were synthesized and evaluated as anaplastic lymphoma kinase inhibitors. Among them, compounds **18a–d** exhibited excellent anti-proliferation activities on H2228 EML4-ALK cancer cell lines with 14–28 nM of the IC_{50} values. In xenograft mouse models, **18a–d** inhibited tumor growth with an excellent inhibitory rate of 75.0% to 86.0% at the dosage of 20 mg kg^{-1} as compared to 72.0% of the reference ceritinib. Using **18d** as a representative, which exhibited the best *in vivo* results, we carried out mechanistic studies such as anti-colony formation, induced tumor cell apoptosis, ALK kinase protein phosphorylation in H2228 tumor cells, and molecular docking. All these results indicate that compound **18d** is a good anti-tumor lead compound and worthy of further study.

Introduction

Anaplastic lymphoma kinase (ALK) is a highly conserved tyrosine receptor kinase (TRK).[1] Research shows that the abnormal expression of ALK, such as gene mutation, rearrangement, and amplification, is closely related to a variety of human malignant tumors (such as neuroblastoma and non-small cell lung cancer).[2,3] In patients with non-small cell lung cancer (NSCLC), about 5% are accompanied by ALK and EML4 (echinoderm microtubule-associated protein-like 4) gene fusion mutation, which activates ALK and multiple downstream signal pathways, resulting in rapid cell proliferation and differentiation, finally leading to the occurrence of tumors.[4,5] Thus, ALK is one of the hot targets in anti-tumor drug development. In 2011, the first drug for NSCLC treatment with ALK-positive crizotinib was approved by FDA.[6] Subsequently, second-generation ALK inhibitors with stronger specificity and affinity for ALK kinase, such as ceritinib[7] and brigatinib,[8] were also launched successively. Although they are indispensable in saving the lives of cancer patients, drug resistance inevitably occurs after long-term use due to various reasons.[9,10] Therefore, it is of great significance to develop new drug molecules with good anti-tumor activity and minimal side effects.

Sulfoxide compounds also exhibit chirality when their sulfur atoms are linked with two different groups.[11] Although most chiral research focuses on chiral carbon compounds, chiral sulfoxides have also received extensive attention in the development of some important drugs.[12,13] For example, omeprazole, a drug for treating stomach diseases, has a sulfoxide structure and was marketed in the form of a racemate in the early stages for clinical use. The (−)-isomer of omeprazole is mainly metabolized by CYP3A4, whereas the (+)-isomer is mainly metabolized by CYP2C19. Considering the obvious expression difference of the CYP2C19 metabolic enzyme in the population, esomeprazole, the (−)-isomer of omeprazole, was launched in 2001 as a sole component[14] to ensure the safety of individual drug use and is still among the top 200 globally sold drugs. In addition, potassium ion channel inhibitor aprikalim,[15] antiplatelet aggregation molecule OPC-29030,[16,17] glutathione synthesis inhibitor L-butyronine sulfoximine,[18] and anticancer drug AZD6738 (ref. 19) are all chiral sulfoxide derivatives (Fig. 1).

From the structures of second-generation ALK inhibitors such as ceritinib, brigatinib, TAE684,[20] and ASP-3026,[21] we found that they share similar skeletal structures, such as pyrimidine ring cores and aniline moiety linked with cyclic

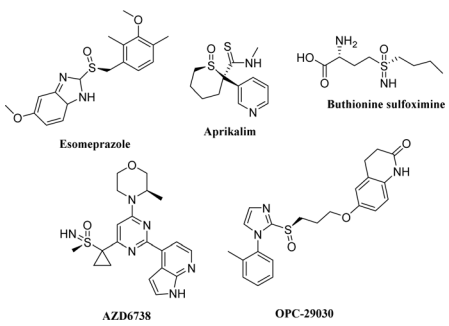

Fig. 1 Drugs containing sulfoxide.

School of Pharmaceutical Sciences, Sun Yat-sen University, Guangzhou 510006, China. E-mail: lixsh@mail.sysu.edu.cn

† Electronic supplementary information (ESI) available. See DOI: https://doi.org/10.1039/d4ra01556h

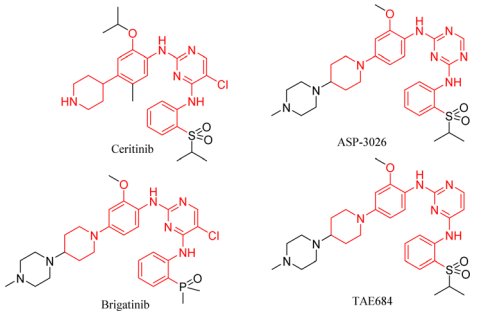

Fig. 2 Representative ALK inhibitors.

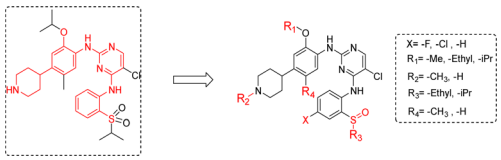

Fig. 3 The modification strategy of the new ALK inhibitors.

aliphatic amino groups (Fig. 2). Investigations indicated that ceritinib has higher metabolic stability and fewer toxic side effects as compared to molecules such as ASP-3026 with amino groups at the 1- and 4-positions of the phenyl ring.[12] Considering drug design and structure–activity studies, small changes in molecular structure often lead to huge differences in their activities, therefore, we chose ceritinib for further structural modification, hoping to get a new lead compound with better activity and fewer side effects.

Our modification strategy for new ALK inhibitors is shown in Fig. 3. Firstly, considering the characteristics and potential chirality of sulfoxide groups, we replaced the sulfone structure in ceritinib with sulfoxide and simultaneously screened the effects of different alkyl groups R_3 on activity. Halogen atoms, such as fluorine, have strong electronegativity, small atomic radius, and good lipophilicity;[22] therefore, introducing fluorine atoms into drug molecules can adjust the lipophilicity of molecules, further affecting the affinity, pharmacokinetics, and bioavailability of drug molecules with targets.[23,24] Therefore, we substituted fluorine and chlorine in the *m*-position of the sulfoxide group, expecting candidate compounds with superior activity. We also explored the effects of other structural sites, such as different alkoxy groups (R_1), on the benzene ring, different groups on the nitrogen atom of piperidine (R_2), and alkyl substitution on the benzene ring (R_4), on anti-tumor activity.

Experimental

Chemistry

Reagents and conditions. All reagents used in the synthesis were obtained commercially and were used without further purification unless otherwise specified. The ^{1}H NMR and ^{13}C NMR spectra were recorded using TMS as the internal standard on a Bruker BioSpin GmbH spectrometer at 400/500 and 100/125 MHz, respectively. High-resolution mass spectra (HR-MS) were obtained using a Shimadzu LCMS-ITTOF mass spectrometer. The reactions were monitored by thin-layer chromatography (TLC) on glass-packed precoated silica gel plates and visualized in an iodine chamber or with a UV lamp. Flash column chromatography was performed using silica gel (200–300 mesh) purchased from Qingdao Haiyang Chemical Co. Ltd Chemicals and solvents were of reagent grade and used without further purification. The purities of all the final synthesized compounds were ≥95% as determined by high-performance liquid chromatography (HPLC).

The general method for the synthesis of intermediates ***2a–b.*** Starting material **1** (10 mmol) was dissolved in 20 mL of sodium hydroxide aqueous solution (5 mol L^{-1}), heated to reflux, and monitored with TLC. After the reaction was completed, hydrochloric acid (1 mol L^{-1}) was added to adjust the pH to 6–7. The precipitate was filtered and dried to obtain the product.

*2-Amino-5-fluorobenzenethiol (**2a**).* Yellow-green solid. 50.3% yield. ^{1}H NMR (400 MHz, chloroform-*d*) δ 7.01–6.82 (m, 2H), 6.67 (dd, J = 8.5, 4.7 Hz, 1H), 4.19 (s, 2H).

*2-Amino-5-chlorobenzenethiol (**2b**).* Light-green solid. 58.7% yield. ^{1}H NMR (400 MHz, chloroform-*d*) δ 7.23–6.95 (m, 2H), 6.65 (d, J = 8.6 Hz, 1H), 4.32 (s, 2H).

The general method for the synthesis of intermediates ***3a–d.*** The intermediate **2a–c** (10 mmol) was dissolved in methanol (20 mL), and then potassium hydroxide solid (20 mmol, 5.6 g), and bromoethane or 2-bromopropane (12 mmol) were added in turn. The reaction mixture was stirred overnight at room temperature. After TLC confirmed that the reaction was complete, the solvent was removed under a vacuum, and 15 mL of water was added, followed by extraction with dichloromethane (30 mL × 2). The combined organic phase was washed with brine, dried with anhydrous sodium sulfate, and the solvent was removed under reduced pressure to obtain the crude product, which was purified by silica gel column chromatography (petroleum ether as eluent : ethyl acetate = 30–20 : 1) to obtain the intermediates **3a–d**.

*2-(Ethylthio)aniline (**3a**).* Light yellow oil. 95.5% yield. ^{1}H NMR (400 MHz, chloroform-*d*) δ 7.41 (dd, J = 7.6, 1.3 Hz, 1H), 7.14 (td, J = 8.0, 1.5 Hz, 1H), 6.80–6.62 (m, 2H), 4.37 (s, 2H), 2.79 (q, J = 7.3 Hz, 2H), 1.26 (t, J = 7.3 Hz, 3H).

*2-(Isopropylthio)aniline (**3b**).* Light yellow oil. 91.2% yield. ^{1}H NMR (400 MHz, chloroform-*d*) δ 7.41 (dd, J = 7.6, 1.3 Hz, 1H), 7.14 (td, J = 8.0, 1.5 Hz, 1H), 6.80–6.62 (m, 2H), 4.33 (s, 2H), 3.06–3.09 (m, 1H), 1.29–1.26 (d, J = 7.3 Hz, 6H).

*2-(Ethylthio)-4-fluoroaniline (**3c**).* Light yellow oil. 87.9% yield. ^{1}H NMR (400 MHz, $CDCl_3$) δ 7.05–6.89 (m, 2H), 6.72–6.53 (m, 1H), 4.74 (s, 2H), 3.40–2.94 (m, 2H), 1.22 (t, J = 7.5 Hz, 3H).

*4-Chloro-2-(ethylthio)aniline (**3d**).* Light yellow oil. 85.3% yield. ^{1}H NMR (400 MHz, chloroform-*d*) δ 7.00–6.59 (m, 2H), 6.42–6.23 (m, 1H), 4.53 (s, 2H), 3.05–2.77 (m, 2H), 1.25 (t, J = 7.2 Hz, 3H).

The general method for the synthesis of intermediates ***4a–d.*** With the synthesis of intermediate **4a** as an example, **3a**

(10 mmol, 1.53 g) was dissolved in 5 mL of acetic acid, and then 30% hydrogen peroxide solution (1.25 g, 11 mmol) was slowly added at 0 °C. The mixture was stirred at the same temperature for 30 minutes, and then at room temperature for 4–5 hours. Sodium hydroxide (3.5 g) in crushed ice was added to the reaction system and stirred for 5 minutes. The mixture was extracted twice with 30 mL of dichloromethane. The organic phase was combined, washed with brine, and dried with anhydrous sodium sulfate. The solvent was removed under a vacuum and purified by silica gel column chromatography (petroleum ether : ethyl acetate = 8 : 1 to 2 : 1) to afford 1.56 g of yellowish oil product. Yield: 92%.

^{1}H NMR (400 MHz, DMSO-d_6) δ 7.27 (d, J = 7.9 Hz, 1H), 7.20 (t, J = 7.8 Hz, 1H), 6.71 (dd, J = 18.1, 8.1 Hz, 2H), 5.63 (s, 2H), 2.94 (tq, J = 13.2, 6.6 Hz, 2H), 1.06 (t, J = 7.6 Hz, 3H).

*The general method for the synthesis of intermediates **5a–d**.* With the synthesis of intermediate **5a** as an example, to the solution of intermediate **4a** (10 mmol, 1.7 g) in dry DMF (30 mL), sodium hydride (60 wt%, 25 mmol, 1 g, 2.5 eq.) was added at 0 °C. The mixture was stirred for 15 minutes, and 2,4,5-trichloropyrimidine (20 mmol, 3.62 g) in dry DMF (10 mL) was added dropwise within 1 hour. The mixture was stirred at room temperature overnight. Water 30 mL was added, and the mixture was extracted with ethyl acetate (3 × 30 mL). The combined organic phase was washed with water and brine, dried over anhydrous sodium sulfate, concentrated to obtain the crude product, which was purified in silica gel column chromatography (petroleum ether : ethyl acetate = 10 : 1 to 4 : 1) to obtain 1.92 g of light-yellow solid product. Yield: 61%. ^{1}H NMR (400 MHz, chloroform-d) δ 11.03 (s, 1H), 8.62 (d, J = 8.5 Hz, 1H), 8.25 (d, J = 1.3 Hz, 1H), 7.58 (t, J = 7.9 Hz, 1H), 7.31 (dd, J = 7.7, 1.7 Hz, 1H), 7.19 (t, J = 7.5 Hz, 1H), 3.29–2.81 (m, 2H), 1.27 (td, J = 7.6, 1.2 Hz, 3H).

*The general method for the synthesis of intermediates **7a–d**.* With the synthesis of intermediate **7b** as an example, caesium carbonate (30 mmol, 9.77 g) was added to a solution (25 mL) of starting material 6 (20 mmol, 3.78 g) in isopropanol. The mixture was refluxed for 10 hours. After the reaction was completed, the solvent was removed under a vacuum. Water (20 mL) was added to the residue and then extracted with dichloromethane (30 mL × 2). The combined organic phase was washed with brine and dried with anhydrous sodium sulfate. The solvent was removed to obtain 3.8 g of the orange solid product. Yield: 83%. ^{1}H NMR (400 MHz, chloroform-d) δ 7.72 (d, J = 7.5 Hz, 1H), 7.09 (d, J = 7.9 Hz, 1H), 4.63 (dt, J = 13.8, 6.1 Hz, 1H), 2.36 (d, J = 7.9 Hz, 3H), 1.41 (t, J = 7.0 Hz, 6H).

*The general method for the synthesis of intermediates **8a–d**.* With the synthesis of intermediate **8b** as an example, to the solution of intermediate **7b** (10 mmol, 2.29 g) in 1,4-dioxane (30 mL), potassium carbonate solid (25 mmol, 3.46 g), bis triphenylphosphine palladium(II) chloride (210.6 mg, 0.3 mmol), 4-pyridine boric acid (12 mmol, 1.48 g), and 10 mL of water were added in turn. The reaction was refluxed under nitrogen protection for 8 hours. After the reaction finished, the solvent was removed under a vacuum. Water was added to the residue and the mixture was extracted with dichloromethane (40 mL × 3). The combined organic phase was washed with brine and dried with anhydrous sodium sulfate. The solvent was removed under a vacuum to obtain the crude product, which was purified by silica gel column chromatography (petroleum ether : ethyl acetate : dichloromethane/8 : 2 : 1) to obtain 2.55 g of a yellow solid. Yield: 93%. ^{1}H NMR (400 MHz, chloroform-d) δ 8.61 (d, J = 6.1 Hz, 2H), 7.27 (d, J = 6.1 Hz, 2H), 6.68 (d, J = 18.5 Hz, 2H), 4.53 (p, J = 6.0 Hz, 1H), 2.21 (s, 3H), 1.38 (d, J = 6.1 Hz, 6H).

*The general method for the synthesis of intermediates **9a–d** and **10a–d**.* The syntheses of intermediates **9b** and **10b** are used as examples. To a solution of intermediate **8b** (10 mmol, 2.72 g) in 15 mL acetonitrile, iodomethane (15 mmol, 2.15 g) was added. After stirring at 50 °C for 3 hours, the solvent was removed under a vacuum. The crude product **9b** was used directly for the next step.

To a solution of crude product **9b** in 20 mL of methanol, sodium borohydride (40 mmol, 1.51 g) was added in batches in an ice bath. The reaction was stirred for half an hour, and then at room temperature for 2 hours. A saturated ammonium chloride solution was added to the reaction system to quench the reaction, the solvent was removed under reduced pressure. Water (30 mL) was added to the residue and then extracted with dichloromethane (30 mL × 3). The combined organic phase was washed with brine and dried with anhydrous sodium sulfate. The solvent was removed under a vacuum and the crude product was purified by column chromatography (dichloromethane : methanol = 50 : 1 to 20 : 1) to obtain 2.1 g of yellowish oily product. Yield: 72%. ^{1}H NMR (400 MHz, chloroform-d) δ 7.61 (s, 1H), 6.81 (s, 1H), 5.60 (s, 1H), 4.59 (dq, J = 12.1, 6.2 Hz, 1H), 3.10 (q, J = 2.8 Hz, 2H), 2.66 (t, J = 5.6 Hz, 2H), 2.41 (d, J = 16.5 Hz, 4H), 2.24 (s, 3H), 1.64 (s, 1H), 1.36 (d, J = 6.0 Hz, 6H).

*The general method for the synthesis of intermediates **11a–d**.* With the synthesis of intermediate **11b** as an example, tin(IV) chloride dihydrate (50 mmol, 10.11 g) was added to the solution of intermediate **10b** (10 mmol, 2.6 g) in dichloromethane/methanol (40 mL, v/v, 1 : 1). The mixture was stirred, and hydrochloric acid (6.7 mL) was added in drops. After the reaction was stirred and refluxed at 50 °C for 5 hours, ammonia water was used to adjust the pH to 5, and then to 9 with solid sodium carbonate. This was followed by filtration with diatomite and washing the filter cake with a mixture of dichloromethane : methanol = 1 : 1. The solvent was removed under a vacuum to afford the crude product, which was purified by column chromatography (dichloromethane : methanol = 50 : 1 to 20 : 1) to obtain a bright yellow solid product. ^{1}H NMR (400 MHz, chloroform-d) δ 7.61 (s, 1H), 6.81 (s, 1H), 5.60 (s, 1H), 4.59 (m, J = 12.1, 6.2 Hz, 1H), 3.10 (q, J = 2.8 Hz, 2H), 2.66 (t, J = 5.6 Hz, 2H), 2.41 (d, J = 16.5 Hz, 4H), 2.24 (s, 3H), 1.64 (s, 1H), 1.36 (d, J = 6.0 Hz, 6H).

*The general method for the synthesis of intermediates **12a–d**.* With the synthesis of intermediate **12b** as an example, to a solution of intermediate **11b** (5 mmol, 1.45 g) in methanol (5 mL), 10% palladium carbon (150 mg) was added. The reaction was carried out at 50 °C in a hydrogen atmosphere at a pressure of 40 bar. After 24 h, the temperature was decreased to room temperature. The mixture was filtered with diatomaceous earth and the cake was washed twice with anhydrous ethanol (10 mL × 2). The solvent was removed, and the crude product was

purified with silica gel column chromatography to obtain a light-yellow oil-free substance.

^{1}H NMR (400 MHz, chloroform-*d*) δ 6.73 (s, 1H), 6.53 (s, 1H), 4.44 (*p*, J = 6.1 Hz, 1H), 3.62 (s, 2H), 2.98 (d, J = 11.5 Hz, 2H), 2.60 (*p*, J = 8.1, 7.6 Hz, 1H), 2.34 (s, 3H), 2.21 (s, 3H), 2.07 (dd, J = 15.0, 11.2 Hz, 2H), 1.83–1.64 (m, 4H), 1.33 (d, J = 6.1 Hz, 6H).

*The general procedure for the synthesis of target compounds **18a–l**.* With the synthesis of intermediate **18b** as an example, to a solution of intermediate **12b** (1 mmol, 262 mg, 1 eq.) in 10 mL of isopropanol, intermediate **5b** (2 mmol, 630 mg, 2 eq.) and trifluoroacetic acid (2 mmol, 2 eq.) were added. The reaction was heated and refluxed for 8 hours, and isopropanol was removed under a vacuum. Then, a 10% sodium hydroxide aqueous solution was added to adjust the pH to 10, and dichloromethane (30 mL × 3) was used for extraction. The combined organic phase was washed with brine, dried with anhydrous sodium sulfate, and concentrated under reduced pressure. The crude product was purified by silica gel column chromatography (ethyl acetate : petroleum ether = 1 : 2–3 : 1) to obtain a yellowish solid.

*4-Chloro-N2-(2-isopropoxy-5-methyl-4-(piperidin-4-yl)phenyl)-N5-(2-(isopropylsulfinyl)phenyl)pyrimidine-2,5-diamine (**18a**).* Pale yellow solid, yield: 39.8%, HPLC (peak area normalization method) purity 97.08%, HPLC conditions: 1 mL min^{-1} gradient elution MeCN : H_2O = 90 : 10 → 10 : 90 (0.1% Et_3N in each component), t_R = 1.481 min. ^{1}H NMR (400 MHz, chloroform-*d*) δ 10.25 (s, 1H), 8.59 (d, J = 8.3 Hz, 1H), 8.10 (d, J = 28.3 Hz, 2H), 7.52 (s, 2H), 7.38 (d, J = 7.7 Hz, 1H), 7.16 (t, J = 7.5 Hz, 1H), 6.82 (s, 1H), 4.65–4.44 (m, 1H), 3.39 (dq, J = 13.7, 6.7 Hz, 1H), 3.21 (d, J = 5.5 Hz, 2H), 2.89–2.72 (m, 3H), 2.20 (s, 3H), 1.77–1.56 (m, 5H), 1.42 (d, J = 6.9 Hz, 3H), 1.38 (d, J = 6.0 Hz, 6H), 1.15 (d, J = 6.8 Hz, 3H). ^{13}C NMR (101 MHz, $CDCl_3$) δ 157.54, 155.61, 155.03, 144.69, 140.89, 138.05, 132.03, 128.30, 127.56, 126.76, 126.29, 123.86, 122.45, 120.72, 111.00, 105.77, 71.44, 52.63, 47.40, 38.50, 33.85, 22.28, 18.92, 16.50, 16.11. HR-ESI-MS for $C_{28}H_{36}ClN_5O_2S$ ([M + Na]$^+$) calcd: 564.2170; Found: 564.2161. FT-IR (KBr) ν(–N–H) 3413.05 cm^{-1}; ν(–C–H): 2972.59 cm^{-1}, 2928.43 cm^{-1}; ν(–S=O): 1111.09 cm^{-1}; ν(–C–Cl) 734.06 cm^{-1}. Elemental analysis: analysis calculated for $C_{28}H_{36}ClN_5O_2S$, C, 62.03; H, 6.69; Cl, 6.54; N, 12.92; O, 5.90; S, 5.91; observed, C, 61.86, H, 6.75, N, 13.06, S, 5.98.

*4-Chloro-N2-(2-isopropoxy-5-methyl-4-(1-methylpiperidin-4-yl) phenyl)-N5-(2-(isopropylsulfinyl)phenyl)pyrimidine-2,5-diamine (**18b**).* Pale yellow solid, yield: 48.1%, HPLC (peak area normalization method) purity 98.00%, HPLC conditions: 1 mL min^{-1} gradient elution MeCN : H_2O = 90 : 10 → 10 : 90 (0.1% Et_3N in each component), t_R = 1.497 min. ^{1}H NMR (400 MHz, chloroform-*d*) δ 10.25 (s, 1H), 8.59 (d, J = 8.4 Hz, 1H), 8.10 (d, J = 28.4 Hz, 2H), 7.51 (s, 2H), 7.38 (d, J = 7.6 Hz, 1H), 7.15 (t, J = 7.5 Hz, 1H), 6.82 (s, 1H), 4.53 (*p*, J = 6.1 Hz, 1H), 3.38 (*p*, J = 6.8 Hz, 1H), 3.00 (d, J = 8.5 Hz, 2H), 2.66 (q, J = 9.3, 8.1 Hz, 1H), 2.36 (s, 3H), 2.19 (s, 3H), 2.15–2.01 (m, 2H), 1.83–1.71 (m, 4H), 1.42 (d, J = 6.9 Hz, 3H), 1.37 (d, J = 6.0 Hz, 6H), 1.15 (d, J = 6.8 Hz, 3H). ^{13}C NMR (101 MHz, $CDCl_3$) δ 157.53, 155.59, 155.02, 144.66, 140.90, 137.57, 132.02, 128.28, 127.50, 126.83, 126.27, 123.84, 122.42, 120.67, 110.73, 105.75, 71.29, 56.59, 52.63, 46.54, 37.38, 33.00, 22.27, 18.92, 16.49, 16.10. HR-ESI-MS for $C_{29}H_{38}ClN_5O_2S$ ([M + H]$^+$) calcd: 556.2508; found: 556.2579. FT-IR (KBr) ν(–N–H) 3416.35 cm^{-1}; ν(–C–H): 2972.95 cm^{-1}, 2933.48 cm^{-1}; ν(–S=O): 1112.45 cm^{-1} ν(–C–Cl) 760.35 cm^{-1}. Elemental analysis: analysis calculated for $C_{29}H_{38}ClN_5O_2S$, C, 62.63; H, 6.89; Cl, 6.37; N, 12.59; O, 5.75; S, 5.76; observed, C, 62.56, H, 7.01, N, 13.46, S, 5.98.

*4-Chloro-N5-(2-(ethylsulfinyl)phenyl)-N2-(2-isopropoxy-5-methyl-4-(piperidin-4-yl)phenyl)pyrimidine-2,5-diamine (**18c**).* Pale yellow solid, yield: 40.2%, HPLC (peak area normalization method) purity 97.26%, HPLC conditions: 1 mL min^{-1} gradient elution MeCN : H_2O = 90 : 10 → 10 : 90 (0.1% Et_3N in each component), t_R = 1.046 min. ^{1}H NMR (400 MHz, chloroform-*d*) δ 10.06 (s, 1H), 8.54 (d, J = 8.3 Hz, 1H), 8.08 (d, J = 36.3 Hz, 2H), 7.57–7.33 (m, 3H), 7.16 (t, J = 7.5 Hz, 1H), 6.80 (s, 1H), 4.54 (*p*, J = 6.0 Hz, 1H), 3.13 (ddd, J = 43.9, 12.9, 7.4 Hz, 4H), 2.77 (ddt, J = 11.2, 6.0, 2.9 Hz, 3H), 2.18 (s, 3H), 1.75 (d, J = 9.4 Hz, 5H), 1.36 (d, J = 6.1 Hz, 6H), 1.26 (t, J = 7.5 Hz, 3H). ^{13}C NMR (101 MHz, $CDCl_3$) δ 157.55, 155.70, 155.09, 144.68, 140.48, 138.00, 132.14, 127.81, 127.56, 127.27, 126.78, 123.97, 122.89, 120.67, 110.99, 105.75, 71.46, 47.36, 47.29, 38.46, 33.77, 22.28, 18.91, 7.58. HR-ESI-MS for $C_{27}H_{34}ClN_5O_2S$ ([M–H]$^-$) calcd: 526.2049; found: 526.2109. FT-IR (KBr) ν(–N–H) 3414.36 cm^{-1}; ν(–C–H): 2974.32 cm^{-1}, 2931.76 cm^{-1}; ν(–S=O): 1111.54 cm^{-1} ν(–C–Cl) 753.04 cm^{-1}. Elemental analysis: analysis calculated for $C_{27}H_{34}ClN_5O_2S$, C, 61.41; H, 6.49; Cl, 6.71; N, 13.26; O, 6.06; S, 6.07; observed, C, 60.86, H, 6.44, N, 13.36, S, 6.28.

*4-Chloro-N5-(2-(ethylsulfinyl)phenyl)-N2-(2-isopropoxy-5-methyl-4-(1-methylpiperidin-4-yl)phenyl)pyrimidine-2,5-diamine (**18d**).* Pale yellow solid, yield: 44.3%, HPLC (peak area normalization method) purity 97.00%, HPLC conditions: 1 mL min^{-1} gradient elution MeCN : H_2O = 90 : 10 → 10 : 90 (0.1% Et_3N in each component), t_R = 0.936 min. ^{1}H NMR (400 MHz, chloroform-*d*) δ 9.98 (s, 1H), 8.53–8.35 (m, 1H), 8.00 (d, J = 37.2 Hz, 2H), 7.57–7.36 (m, 2H), 7.32 (d, J = 7.6 Hz, 1H), 7.09 (t, J = 7.5 Hz, 1H), 6.72 (s, 1H), 4.50 (dq, J = 12.1, 6.0 Hz, 1H), 3.26 (d, J = 9.9 Hz, 2H), 3.17–2.93 (m, 2H), 2.74–2.58 (m, 1H), 2.45 (s, 3H), 2.34 (t, J = 12.2 Hz, 2H), 2.08 (s, 3H), 1.91 (d, J = 12.0 Hz, 2H), 1.73 (t, J = 12.9 Hz, 2H), 1.29 (d, J = 6.0 Hz, 6H), 1.17 (t, J = 7.5 Hz, 3H). ^{13}C NMR (101 MHz, $CDCl_3$) δ 157.51, 155.55, 155.30, 144.77, 138.80, 137.86, 131.92, 129.84, 128.33, 127.30, 126.80, 126.64, 125.51, 120.68, 110.74, 105.64, 71.30, 56.58, 47.52, 46.54, 37.38, 33.01, 32.97, 22.26, 18.92, 7.42. and HR-ESI-MS for $C_{28}H_{36}ClN_5O_2S$ ([M + H]$^+$) calcd: 514.0815; found: 514.0994. FT-IR (KBr) ν(–N–H) 3415.67 cm^{-1}; ν(–C–H): 2973.92 cm^{-1}, 2934.78 cm^{-1}; ν(–S=O): 1111.85 cm^{-1} ν(–C–Cl) 775.55 cm^{-1}. Elemental analysis: analysis calculated for $C_{28}H_{36}ClN_5O_2S$, C, 62.03; H, 6.69; Cl, 6.54; N, 12.92; O, 5.90; S, 5.91; observed, C, 61.86, H, 6.84, N, 12.76, S, 6.28.

*4-Chloro-N5-(2-(ethylsulfinyl)phenyl)-N2-(2-methoxy-5-methyl-4-(1-methylpiperidin-4-yl)phenyl)pyrimidine-2,5-diamine (**18e**).* Pale yellow solid, yield: 50.1%, HPLC (peak area normalization method) purity 98.34%, HPLC conditions: 1 mL min^{-1} gradient elution MeCN : H_2O = 90 : 10 → 10 : 90 (0.1% Et_3N in each component), t_R = 1.253 min. ^{1}H NMR (400 MHz, chloroform-*d*)

δ 10.10 (s, 1H), 8.55 (d, J = 8.3 Hz, 1H), 8.14 (s, 1H), 8.04 (s, 1H), 7.51 (dd, J = 16.4, 9.2 Hz, 2H), 7.45–7.35 (m, 1H), 7.17 (t, J = 7.9 Hz, 1H), 6.81 (s, 1H), 3.86 (s, 3H), 3.11–3.02 (m, 2H), 2.49 (s, 3H), 2.29 (t, J = 12.0 Hz, 3H), 2.21 (s, 3H), 2.03–1.88 (m, 3H), 1.82 (t, J = 11.6 Hz, 3H), 1.27 (t, J = 7.4 Hz, 3H). ^{13}C NMR (101 MHz, $CDCl_3$) δ 157.58, 155.69, 155.04, 146.75, 140.53, 136.83, 132.14, 127.65, 127.28, 126.70, 123.84, 122.85, 120.74, 117.17, 108.20, 107.68, 106.03, 56.26, 55.76, 47.30, 45.70, 36.89, 32.11, 18.90, 8.97, 7.59. HR-ESI-MS for $C_{26}H_{32}ClN_5O_2S$ ($[M + H]^+$) calcd: 532.0753; found: 532.0714.

4-Chloro-N5-(2-(ethylsulfinyl)-4-fluorophenyl)-N2-(2-methoxy-5-methyl-4-(1-methylpiperidin-4-yl)phenyl)pyrimidine-2,5-diamine ***(18f).*** Pale yellow solid, yield: 47.7%, HPLC (peak area normalization method) purity 98.26%, HPLC conditions: 1 mL min^{-1} gradient elution MeCN : H_2O = 90 : 10 → 10 : 90 (0.1% Et_3N in each component), t_R = 0.811 min. ^{1}H NMR (400 MHz, chloroform-*d*) δ 9.41 (s, 1H), 8.45–8.34 (m, 1H), 8.13 (s, 1H), 7.92 (s, 1H), 7.46 (s, 1H), 7.23 (d, J = 7.4 Hz, 2H), 6.81 (s, 1H), 3.86 (s, 3H), 3.11 (td, J = 13.5, 5.5 Hz, 4H), 2.94 (q, J = 7.4 Hz, 1H), 2.42 (s, 3H), 2.19 (s, 3H), 1.95–1.73 (m, 6H), 1.28 (d, J = 7.5 Hz, 3H). ^{13}C NMR (101 MHz, chloroform-*d*) δ 159.56, 157.56 (d, J_{1C-F} = 251.49 Hz), 157.08, 157.08, 155.83, 146.76, 136.89, 135.56 (d, J_{4C-F} = 2.9 Hz), 131.58 (d, J_{3C-F} = 5.6 Hz), 126.73 (t, J_{3C-F} = 10.9), 120.69, 118.81 (d, J_{2C-F} = 22.1 Hz), 113.73 (d, J_{2C-F} = 24.6 Hz), 107.69, 105.58, 55.83, 47.47, 46.08, 37.52, 31.80, 18.90, 7.17. HR-ESI-MS for $C_{26}H_{31}ClFN_5O_2S$ ($[M + Na]^+$) calcd: 564.2170; found: 564.2194.

4-Chloro-N2-(2-ethoxy-5-methyl-4-(1-methylpiperidin-4-yl) phenyl)-N5-(2-(ethylsulfinyl)-4-fluorophenyl)pyrimidine-2,5-diamine ***(18g).*** Pale yellow solid, yield: 49.3%, HPLC (peak area normalization method) purity 99.00%, HPLC conditions: 1 mL min^{-1} gradient elution MeCN : H_2O = 90 : 10 → 10 : 90 (0.1% Et_3N in each component), t_R = 0.814 min. ^{1}H NMR (400 MHz, chloroform-*d*) δ 9.39 (s, 1H), 8.38 (dd, J = 8.8, 4.6 Hz, 1H), 8.13 (s, 1H), 7.91 (s, 1H), 7.50 (s, 1H), 7.22 (dd, J = 10.5, 7.9 Hz, 2H), 6.80 (s, 1H), 4.08 (q, J = 6.9 Hz, 2H), 3.10 (ddt, J = 21.2, 12.7, 7.3 Hz, 4H), 2.69 (td, J = 11.3, 6.7 Hz, 1H), 2.39 (s, 3H), 2.17 (s, 3H), 1.94–1.66 (m, 6H), 1.44 (t, J = 6.9 Hz, 3H), 1.27 (t, J = 7.4 Hz, 3H). ^{13}C NMR (101 MHz, chloroform-*d*) δ 159.58, 157.58 (d, J_{1C-F} = 249.47), 157.11, 155.84, 145.88, 137.58, 135.50, 131.66, 126.75 (d, J_{3C-F} = 7.1 Hz), 126.52 (d, J_{3C-F} = 9.4 Hz), 120.55, 118.81 (d, J_{2C-F} = 22.2 Hz), 113.70 (d, J_{2C-F} = 24.5 Hz), 108.82, 105.32, 64.27, 56.49, 47.46, 46.35, 37.31, 32.72, 18.89, 14.99, 7.15. HR-ESI-MS for $C_{27}H_{33}ClN_5O_2S$ ($[M + H]^+$) calcd: 546.2100; found: 546.2191.

4-Chloro-N5-(2-(ethylsulfinyl)-4-fluorophenyl)-N2-(2-methoxy-5-methyl-4-(piperidin-4-yl)phenyl)pyrimidine-2,5-diamine ***(18h).*** Pale yellow solid, yield: 38.2%, HPLC (peak area normalization method) purity 95.07%, HPLC conditions: 1 mL min^{-1} gradient elution MeCN : H_2O = 90 : 10 → 10 : 90 (0.1% Et_3N in each component), t_R = 1.040 min. ^{1}H NMR (400 MHz, chloroform-*d*) δ 9.44 (s, 1H), 8.49–8.31 (m, 1H), 8.14 (s, 1H), 7.95 (s, 1H), 7.47 (s, 1H), 7.24 (d, J = 7.3 Hz, 2H), 6.80 (s, 1H), 3.89 (s, 3H), 3.37 (d, J = 13.5 Hz, 3H), 3.18–3.02 (m, 2H), 2.95–2.76 (m, 3H), 2.20 (s, 3H), 1.91–1.73 (m, 4H), 1.28 (t, J = 7.5 Hz, 3H). ^{13}C NMR (101 MHz, chloroform-d) δ 159.52, 157.61 (d, J_{1C-F} = 254.5), 157.05, 155.80, 146.72, 137.52, 135.59, 126.66 (t, J_{3C-F} = 9.1), 126.38, 120.70, 118.83 (d, J_{2C-F} = 22.3 Hz), 113.72 (d, J_{2C-F} = 24.5 Hz), 108.30, 107.74, 105.49, 56.42, 55.75, 47.46, 46.21, 37.22, 32.57, 18.89, 9.55, 7.19. HR-ESI-MS for $C_{25}H_{29}ClFN_5O_2S$ ($[M + H]^+$) calcd: 518.1787; found: 518.1794.

4-Chloro-N5-(4-chloro-2-(ethylsulfinyl)phenyl)-N2-(2-isopropoxy-5-methyl-4-(1-methylpiperidin-4-yl)phenyl)pyrimidine-2,5-diamine ***(18i).*** Pale yellow solid, yield: 45.4%, HPLC (peak area normalization method) purity 96.62%, HPLC conditions: 1 mL min^{-1} gradient elution MeCN : H_2O = 90 : 10 → 10 : 90 (0.1% Et_3N in each component), t_R = 1.472 min. ^{1}H NMR (400 MHz, chloroform-*d*) δ 9.85 (s, 1H), 8.49 (d, J = 8.8 Hz, 1H), 8.14 (s, 1H), 7.96 (s, 1H), 7.64–7.35 (m, 3H), 6.83 (s, 1H), 4.65–4.43 (m, 1H), 3.29–3.07 (m, 2H), 3.07–2.96 (m, 2H), 2.68 (*p*, J = 8.6, 8.1 Hz, 1H), 2.36 (s, 3H), 2.20 (s, 3H), 2.11 (dd, J = 13.6, 5.0 Hz, 2H), 1.79 (qd, J = 7.8, 5.2, 4.8 Hz, 4H), 1.37 (d, J = 6.1 Hz, 6H), 1.30 (t, J = 7.5 Hz, 3H). ^{13}C NMR (101 MHz, $CDCl_3$) δ 157.51, 155.55, 155.30, 144.77, 138.80, 137.86, 131.92, 129.84, 128.33, 127.30, 126.80, 126.64, 125.51, 120.68, 110.74, 105.64, 71.30, 56.58, 47.52, 46.54, 37.38, 33.01, 22.26, 18.92, 7.42. HR-ESI-MS for $C_{28}H_{35}Cl_2N_5O_2S$ ($[M + H]^+$) calcd: 576.2144; found: 576.2033.

4-Chloro-N5-(2-(ethylsulfinyl)-4-fluorophenyl)-N2-(2-isopropoxy-5-methyl-4-(piperidin-4-yl)phenyl)pyrimidine-2,5-diamine ***(18j).*** Pale yellow solid, yield: 33.7%, HPLC (peak area normalization method) purity 97.28%, HPLC conditions: 1 mL min^{-1} gradient elution MeCN : H_2O = 90 : 10 → 10 : 90 (0.1% Et_3N in each component), t_R = 1.135 min. ^{1}H NMR (400 MHz, chloroform-*d*) δ 9.39 (s, 1H), 8.38 (dd, J = 8.8, 4.8 Hz, 1H), 8.13 (s, 1H), 7.93 (s, 1H), 7.59 (s, 1H), 7.27–7.16 (m, 2H), 6.81 (s, 1H), 4.56 (dt, J = 12.0, 6.0 Hz, 1H), 3.29 (d, J = 9.5 Hz, 2H), 3.11 (dd, J = 14.4, 6.9 Hz, 3H), 2.83 (t, J = 12.1 Hz, 3H), 2.17 (s, 3H), 1.86–1.61 (m, 4H), 1.38 (d, J = 6.0 Hz, 6H), 1.33–1.29 (m, 3H). ^{13}C NMR (101 MHz, chloroform-*d*) δ 159.38, 157.61 (d, J_{1C-F} = 258.56), 156.91, 155.72, 148.24, 140.30, 135.85, 130.78 (d, J_{3C-F} = 5.2 Hz), 126.98, 126.68 (d, J_{3C-F} = 7.0 Hz), 119.22, 118.59 (t, J_{2C-F} = 22.2 Hz), 113.72 (d, J_{2C-F} = 24.5 Hz), 108.67, 105.66, 56.22, 55.63, 47.48, 46.19, 41.63, 33.45, 33.35, 7.30. HR-ESI-MS for $C_{27}H_{33}ClFN_5O_2S$ ($[M + H]^+$) calcd: 546.2100; found: 546.2157.

4-Chloro-N5-(2-(ethylsulfinyl)phenyl)-N2-(2-methoxy-4-(1-methylpiperidin-4-yl)phenyl)pyrimidine-2,5-diamine ***(18k).*** Pale yellow solid, yield: 50.3%, HPLC (peak area normalization method) purity 95.53%, HPLC conditions: 1 mL min^{-1} gradient elution MeCN : H_2O = 90 : 10 → 10 : 90 (0.1% Et_3N in each component), t_R = 0.937 min. ^{1}H NMR (400 MHz, chloroform-*d*) δ 10.15 (s, 1H), 8.51 (d, J = 8.2 Hz, 1H), 8.17 (d, J = 8.7 Hz, 1H), 8.11 (s, 1H), 7.54–7.45 (m, 2H), 7.41–7.32 (m, 1H), 7.16 (t, J = 7.9 Hz, 1H), 6.79–6.71 (m, 2H), 3.88 (s, 3H), 3.26 (d, J = 11.4 Hz, 2H), 3.11 (ddd, J = 45.1, 13.0, 7.5 Hz, 2H), 2.63–2.51 (m, 1H), 2.49 (s, 3H), 2.34 (t, J = 12.9 Hz, 2H), 1.93 (dd, J = 29.6, 11.9 Hz, 4H), 1.24 (d, J = 7.5 Hz, 3H). ^{13}C NMR (101 MHz, $CDCl_3$) δ 157.58, 155.69, 155.04, 146.75, 140.53, 136.83, 132.14, 127.65, 127.28, 126.70, 123.84, 122.85, 120.74, 117.17, 107.68, 106.03, 56.26, 55.76, 47.30, 45.70, 36.89, 32.11, 18.90, 8.97, 7.59. HR-ESI-MS for $C_{25}H_{30}ClN_5O_2S$ ($[M + H]^+$) calcd: 500.1882; found: 500.1942.

*4-Chloro-N5-(2-(ethylsulfinyl)-4-fluorophenyl)-N2-(2-isopropoxy-5-methyl-4-(1-methylpiperidin-4-yl)phenyl)pyrimidine-2,5-diamine (**18l**).* Pale yellow solid, yield: 33.2%. HPLC (peak area normalization method) purity 99.46%, HPLC conditions: 1 mL min^{-1} gradient elution MeCN : H_2O = 90 : 10 → 10 : 90 (0.1% Et_3N in each component), t_R = 1.446 min. ^1H NMR (400 MHz, chloroform-*d*) δ 9.38 (s, 1H), 8.47–8.34 (m, 1H), 8.13 (s, 1H), 7.92 (s, 1H), 7.51 (s, 1H), 7.26–7.17 (m, 2H), 6.82 (s, 1H), 4.53 (dt, J = 12.1, 5.9 Hz, 1H), 3.19–2.95 (m, 4H), 2.74–2.59 (m, 1H), 2.36 (s, 3H), 2.16 (s, 3H), 2.14–2.04 (m, 2H), 1.83–1.70 (m, 4H), 1.37 (d, J = 6.0 Hz, 6H), 1.27 (t, J = 7.3 Hz, 3H). ^{13}C NMR (101 MHz, chloroform-*d*) δ 159.56, 157.55 (d, J_{1C-F} = 243.4), 157.09, 155.82, 144.66, 137.71, 135.58 (d, J_{4C-F} = 2.9 Hz), 131.64 (d, J_{3C-F} = 6.1 Hz), 127.35, 126.73 (t, J_{3C-F} = 7.07 Hz), 120.52, 118.82 (d, J_{2C-F} = 22.1 Hz), 113.72 (d, J_{2C-F} = 24.5 Hz), 110.69, 105.27, 71.29, 56.56, 47.46, 46.51, 37.36, 32.97, 22.25, 18.92, 7.18. HR-ESI-MS for $C_{28}H_{35}ClFN_5O_2S$ ($[M+H]^+$) calcd: 560.2257; found: 560.2352.

Biology

Cell origin and culture conditions

Cell origin. The H2228 cell line, a human non-small cell lung cancer cell line, was bought from Shanghai Cell Bank, Chinese Academy of Sciences. The BaF_3/ALK cell line was from Kyinno Biotechnology Co. LTD (Beijing, China). For human normal cell lines, EA.hy926, HK-2, and L02 were also obtained from Shanghai Cell Bank, Chinese Academy of Sciences.

Cell culture. For cell culture, H2228, HK-2, L02, and BaF_3/ALK cell lines were maintained in RPIM 1640 medium supplemented with 10% FBS (fetal bovine serum). For the H2228 cell culture, we added 1% sodium pyruvate (100 mM, Gibco) and GlutaMAX (1X, Gibco) as a nutritional supplement. EA.hy926 cells were cultivated in DMEM medium, with 10% FBS added. All the above cell lines were in an atmosphere of 37 °C, 5% CO_2, and saturated humidity.

Other biology experiments such as cytotoxicity assays, kinase inhibition assays, cell colony formation, *etc.*, are displayed in the ESI† section.

Results and discussion

Chemistry

The synthesis of target compounds **18a–l** and the corresponding intermediates is shown in Schemes 1–4. Starting from benzo[*d*]thiazol-2-amine derivatives with chlorine or fluorine atoms substituted on the benzene ring, hydrolysis was carried out in the presence of NaOH at reflux temperatures to yield 2-amino-5-fluorobenzenethiol (**2a**) or 2-amino-5-chlorobenzenethiol (**2b**), which reacted with brominated alkanes to give thioether intermediates **3a–d**. Oxidation of **3a–d** with hydrogen peroxide yielded the sulfoxide intermediates **4a–d**. The reaction of **4a–d** with 2,4,5-trichloropyrimidine in the presence of sodium hydride in *N*,*N*-dimethylformamide (DMF) yielded the key intermediates **5a–d** with pyrimidine structures (Scheme 1).

Other key intermediates, 4-(1-methylpiperidin-4-yl)aniline derivatives, were prepared according to the route shown in Scheme 2. Compound 2-chloro-4-fluoro-5-nitrobenzene or 1-chloro-5-fluoro-2-methyl-4-nitrobenzene (**6**) was refluxed in different alcohols in the presence of potassium carbonate to obtain intermediates **7a–d**. Suzuki coupling of **7a–d** with pyridin-4-ylboronic acid was catalyzed by $Pd(PPh_3)Cl_2$, providing intermediates **8a–d**, which reacted with iodomethane to afford intermediates **9a–d**.

After reduction by sodium borohydride, **9a–d** were converted into 1-methyl-4-(4-nitrophenyl)-1,2,3,6-tetrahydropyridine derivatives **(10a–d)**, and then, reduced by tin(II) chloride under acidic conditions to obtain aniline derivatives **11a–d**. Hydrogenation of **11a–d** under palladium carbon ultimately yielded the key intermediates **12a–d**.

Intermediates **17a–d** were used to synthesize compounds containing the piperidine moiety, such as compounds **18b** and **18c**. Except for some differences in starting materials, the synthesis of **17a–d** was similar to that of **12a–d.**

After obtaining the above key intermediates, the target products **18a–l** can be obtained by the reaction of intermediates **5a–d** with intermediates **12a–d** or **17a–d** catalyzed by trifluoroacetic acid in isopropanol at reflux temperature.

Biology

Antiproliferative activity and kinase inhibitory activity. The antiproliferative activities of targeted compounds **18a–l** were evaluated using mouse-derived Ba/F3 cells and human non-small cell lung cancer NCI-H2228 cancer cell lines, both of which have high ALK protein expression and different gene fusion mutations. According to the characteristics of cell suspension and adhesion, we used MTT and CCK-8 assay separately, and with ceritinib as the reference. The results listed

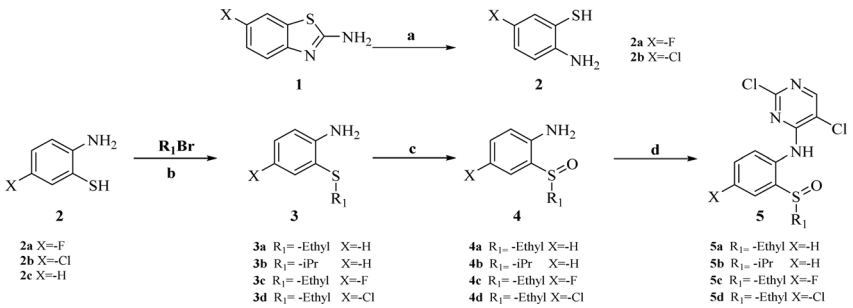

Scheme 1 Synthesis of intermediates **2a**, **2b**, and **5a–d**. Reagents and conditions: (a) NaOH (aq., 2 mol L^{-1}), reflux; (b) NaOH, MeOH, rt. (c) AcOH, H_2O_2, 0 °C. (d) NaH, 2,4,5-trichloropyrimidine, DMF, 0 °C.

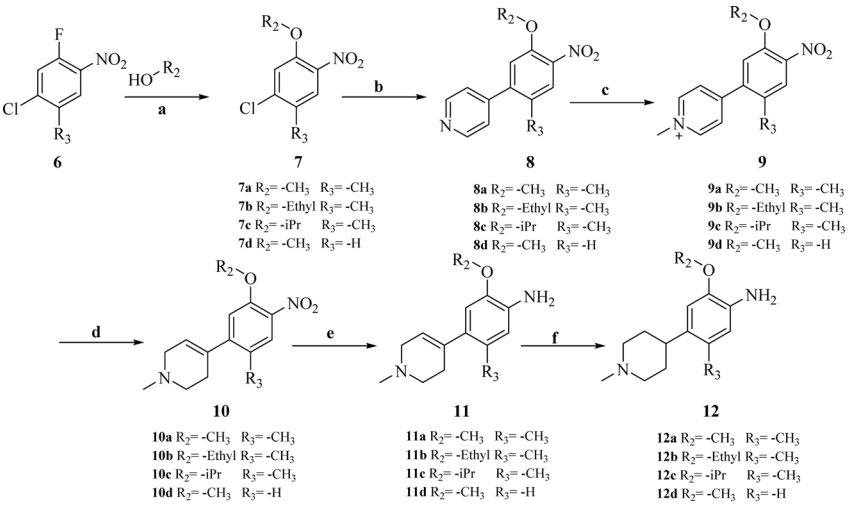

Scheme 2 Synthesis of intermediates **12a–d**. Reagents and conditions: (a) K_2CO_3, reflux. (b) K_2CO_3, pyridin-4-ylboronic acid, $Pd(PPh_3)Cl_2$, dioxane, H_2O. (c) MeCN, MeI. (d) MeOH, $NaBH_4$, 0 °C. (e) $SnCl_2$, HCl, MeOH/DCM = 1 : 1, reflux. (f) 10% Pd/C, H_2, 40 bar, 50 °C.

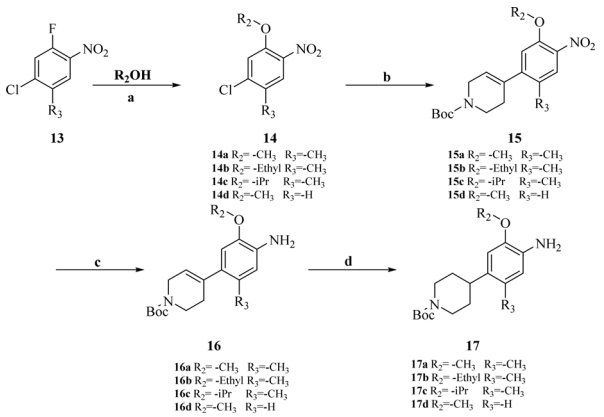

Scheme 3 Synthesis of intermediates **17a–c**. Reagents and conditions: (a) K_2CO_3, reflux. (b) K_2CO_3, (1-(*tert*-butoxycarbonyl)-1,2,3,6-tetrahydropyridin-4-yl)boronic acid $Pd(PPh_3)Cl_2$, dioxane, H_2O. (c) $SnCl_2$, HCl, MeOH/DCM = 1 : 1, reflux. (d) 10% Pd/C, H_2, 40 bar, 50 °C.

in Table 1 indicate that all the target compounds exhibited moderate to good antiproliferative activity; among them, **18a–d** gave a similar or higher activity as compared to the reference.

The structure–activity relationship (SAR) analysis of the target compound indicated the following: (1) when R_1 is ethyl instead of isopropyl, the anti-proliferation effect shows little increase; (2) keeping other structures unchanged, when R_2 is methyl, ethyl, and isopropyl, the efficacy increases sequentially, which may disclose that a group occupying a certain space is preferable here; (3) when R_3 is methyl, its activity is superior to that of hydrogen-substituted compounds on the cell level; (4) the structural difference between compound **18b** and ceritinib is only that the former includes a sulfoxide group, while the latter contains a sulfone structure. However, compound **18d** has better antiproliferative activity against both ALK-overexpressing cells as compared to the reference, indicating that the sulfoxide group is more conducive to improving anti-tumor cell proliferation activity; (5) compounds with fluorine and chlorine atom substituents on the benzene ring exhibit a significant decrease in activity; (6) compounds with R_4 as a -methyl substituent display better inhibition activity than that with hydrogen substitution.

Due to the superior anti-proliferative activity of compounds **18a–d**, we conducted an ALK kinase inhibition activity assay, also with ceritinib as the reference. The results in Table 2 show

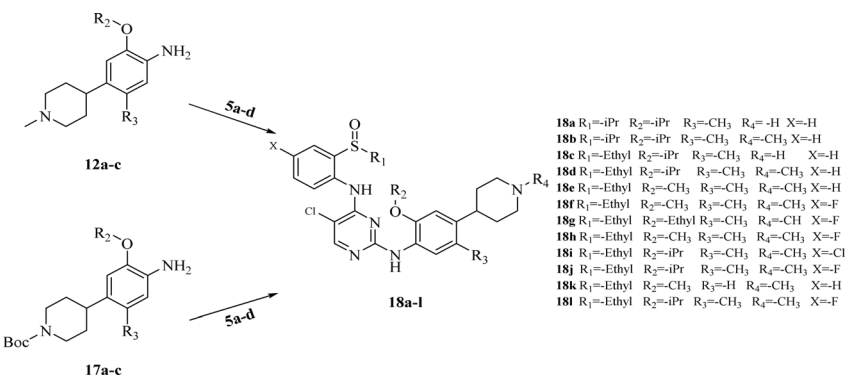

Scheme 4 Synthesis of target compounds **18a–l**. Reagents and conditions: TFA, isopropyl alcohol, reflux.

Table 1 Antiproliferative activities of **18a–l** against H2228 EML4-ALK and BaF_3/NMP-ALK cancer cell lines[a]

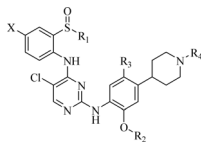

Comp.	R_1	R_2	R_3	R_4	X	H2228 IC_{50} EML4-ALK(nM)	BaF_3/NMP-ALK IC_{50} (nM)
18a	iPr	iPr	Me	H	H	28 ± 8	19 ± 9
18b	iPr	iPr	Me	Me	H	21 ± 6	15 ± 3
18c	Et	iPr	Me	H	H	19 ± 7	11 ± 3
18d	Et	iPr	Me	Me	H	14 ± 6	9 ± 4
18e	Et	Me	Me	Me	H	44 ± 12	33 ± 10
18f	Et	Me	Me	Me	F	37 ± 11	31 ± 13
18g	Et	Et	Me	Me	F	33 ± 7	29 ± 12
18h	Et	Me	Me	H	F	58 ± 16	47 ± 15
18i	Et	iPr	Me	Me	Cl	81 ± 28	77 ± 15
18j	Et	iPr	Me	H	F	63 ± 8	56 ± 4
18k	Et	Me	H	Me	H	57 ± 6	24 ± 5
18L	Et	iPr	Me	Me	F	31 ± 10	28 ± 8
Ceritinib	—	—	—	—	—	25 ± 010	18 ± 1

[a] Experiments repeated independently at least three times.

Table 2 IC_{50} of **18a–d** and ceritinib against ALK kinase[a] units (nM)

Compound	IC_{50} of ALK kinase
18a	3 ± 0.7
18b	1.4 ± 0.2
18c	0.4 ± 0.03
18d	1.2 ± 0.4
Ceritinib	2.4 ± 0.8

[a] Experiments repeated independently at least three times.

that **18b–d** exhibited better activity than ceritinib, which is consistent with the results of anti-proliferation; a slight difference lies with the R_4 group. It seems that 1-methylpiperidine is better at the kinase level. Based on the above anti-tumor cell proliferation activity and kinase inhibition activity tests, we selected **18d** as the representative for further mechanism research.

Compound 18d anti H2228 cell spheroid proliferation and colony formation. The antiproliferation study indicated that **18d** had an IC_{50} of 14.23 nM in the monolayer cell inhibition model; we also assayed the antiproliferation efficacy in the 3D spheroid model. We cultured H2228 cells in a 4% agarose-coated 96-well plate, with 20 000 cells for each well to form spheroids. **18d** presented an inhibitory effect on H2228 spheroids with an IC_{50} of 44.7 nM, which is more than 2 times that of ceritinib.

Clone formation reflects the *in vitro* proliferation ability of tumor cells and their dependence on a colony, which can serve as a supplement to an *in vitro* anti-tumor assay.[25] H2228 cells and BaF3/ALK cells are adherent and suspended cells, respectively. Based on the cell growth characteristics, we used plate cloning and soft agar cloning methods, respectively, for these two types of tumor cells.[26] By processing the colony formation results using corresponding data analysis methods, it was found that **18d** can effectively inhibit the colony formation of two types of tumor cells and present a dose-dependent effect (Fig. 4). By the action of compound **18d** at the concentration of 15 nM, the clone inhibition rates of H2228 and BaF3/ALK cells reached over 70% and over 90%, respectively, and the inhibition of BaF3/ALK cells was more effective, which corresponds with the results in Table 1.

Compound 18d induces tumor cell apoptosis through the mitochondria pathway. Inducing tumor cell apoptosis is one of the mechanisms by which many anticancer drugs produce anti-tumor effects. To evaluate whether compound **18d** is capable of inducing tumor cell apoptosis, we examined H2228 cells using the PI/FITC double staining method in the presence of **18d**. The results in Fig. 5A and B show that compound **18d** can induce the apoptosis of H2228 cancer cell lines, since the ratio of early and late apoptosis cells both increased. Hoechst 33342-stained H2228 cells also displayed high-intensity blue fluorescence, as shown in Fig. 5C. The mitochondrial membrane potential (MMP) in normal cells is closely related to cell physiological functions, and its disorder appears in the early stage of cell apoptosis.[27] Thus, we selected the JC-1 probe to stain the mitochondria of H2228 cells after incubation with compound **18d** for 48 h; the potential of H2228 cells showed significant changes and displayed a high-intensity of green fluorescence.

Compound 18d inhibited the phosphorylation of ALK protein in H2228 tumor cells'.[28,29] In the inhibition assay of the synthesized compounds on ALK kinase, **18d** showed good activity. To further investigate its specific mechanism, we used

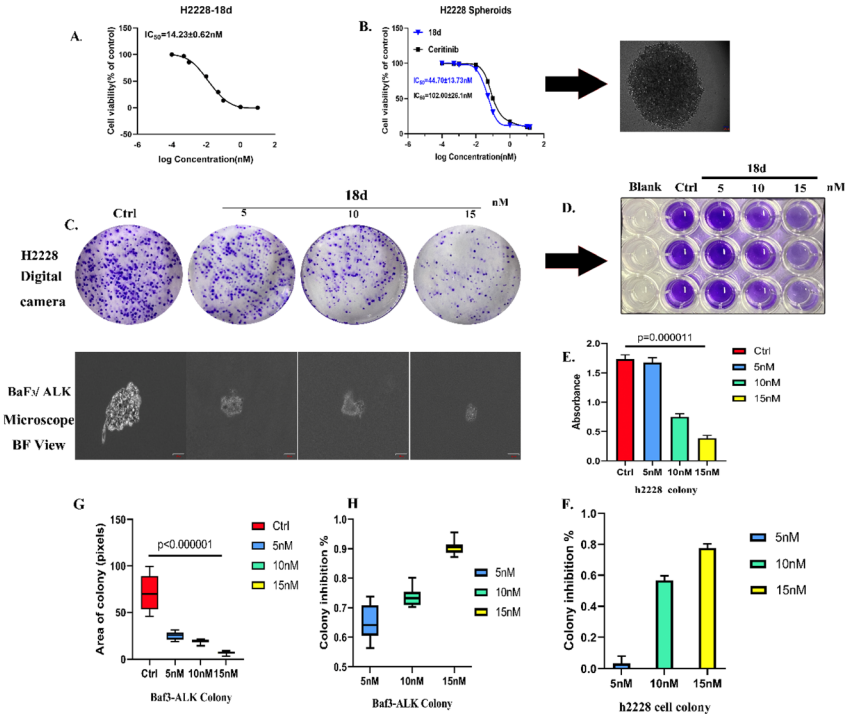

Fig. 4 (A) The concentration of **18d** and the H2228 monolayer model viability curve. (B) The concentration of **18d** or ceritinib and the H2228 spheroid model viability curve; the photograph shows the spheroids under a 4× objective. (C) Representative images of H2228 plate colony formation and BaF3/ALK soft agar colony formation results; the scale bar represents 50 μm and the colony formation images of Baf3 cells were obtained using a 20× objective microscope. (D) 33% acetic acid eluted the color of H2228 cells stained with crystal violet. (E) The absorbance values of each group of H2228 after elution using a microplate reader. (F) The inhibitory effects of compound **18d** at different concentrations calculated using absorbance values of the H2228 cell colony. (G) Ten randomly selected fields of view under a 20× objective; photographs of the formed colony cell clusters were taken and image J was used to calculate the area of the colony sphere. A plot of the size of the colony clusters formed by Baf3-ALK cells under different concentrations of **18d** intervention. (H) The colony inhibition rates of **18d** at various concentrations based on the colony area. The data was shown as mean ± SD and the unpaired two-way *t*-test (assuming all data with the same scatter) was used to determine the levels of significance between comparable samples. $p > 0.05$ was not significant (ns). *$p < 0.05$; **$p < 0.01$; ***$p < 0.001$; ****$p < 0.0001$.

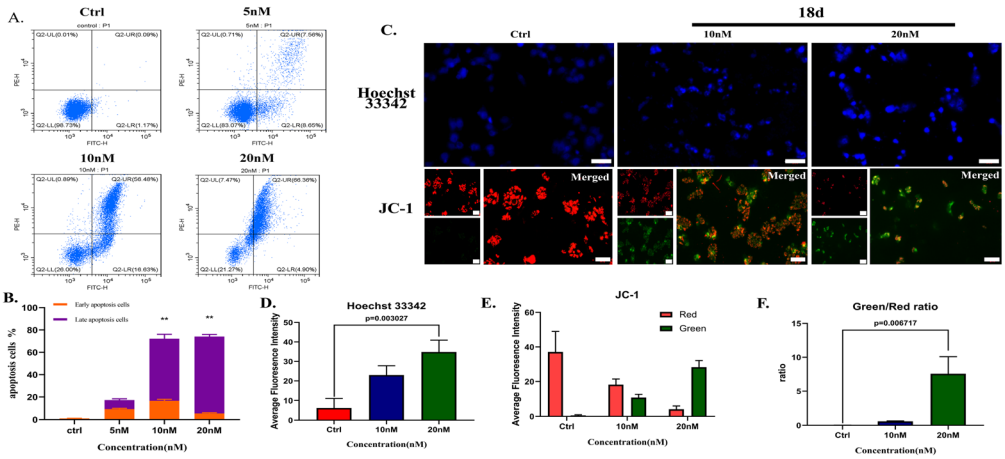

Fig. 5 (A & B) Flow cytometry results and statistics of PI/FITC double staining after treatment with different concentrations of **18d**. (C) H2228 cells cultured with or without **18d** for 48 h, then stained with Hoechst 33342 and photographed by fluorescence microscopy; the scale bar is 50 μm. (D) After JC-1 staining, H2228 cells were observed and photographed using the 10× objective of the fluorescence microscope under the U, B, and G channels; the scale bar is 100 μm. (E) The average fluorescence intensity of green and red channels of each group. (F) The green/red ratio of each group. The data are shown as the mean ± SD, and the unpaired two-way *t*-test (assuming all data with the same scatter) was used to determine the levels of significance between comparison samples. $p > 0.05$ was not significant (ns). *$p < 0.05$; **$p < 0.01$; ***$p < 0.001$; ****$p < 0.0001$.

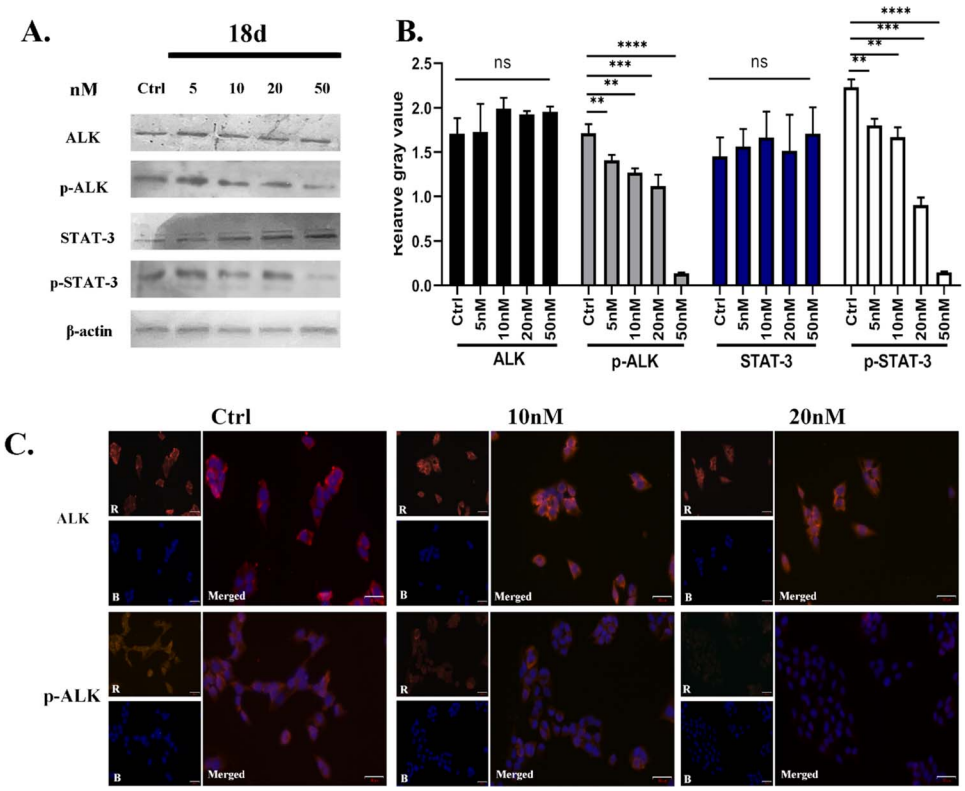

Fig. 6 (A & B) Changes in ALK, p-ALK, STAT-3, and p-STAT-3 protein bands in H2228 cells. (C) The changes in ALK and p-ALK in H2228 cells in the presence of **18d**. The scale bar is 50 μm. The data are shown as the mean ± SD, and the unpaired two-way *t*-test (assuming all data with the same scatter) was used to determine the levels of significance between comparison samples. $p > 0.05$ was not significant (ns). *$p < 0.05$; **$p < 0.01$; ***$p < 0.001$; ****$p < 0.0001$.

the western blot method to assay the protein content in H2228 cells. Fig. 6A and B shows that the interruption of **18d** can reduce the content of p-ALK instead of directly acting on ALK, while p-ALK is the active type of ALK. It also inhibited the activation of the downstream signalling protein STAT-3, since the active form of p-STAT-3 reduces in a dose–response pattern. We also used the immunofluorescence method, which supplied another view to support the western blot findings. The same results were obtained as for the western blot assay, which indicated that **18d** indeed reduced the phosphorylation of ALK.

The effect of 18d on the cycle of H2228 tumor cells. Various studies have found that cell division is vigorous in tumor tissue, and most cells are in the rapid division phase. Therefore, studying the cycle changes of tumor cells after the action of anti-tumor compounds is essential for a comprehensive understanding of the mechanisms of active compounds. To evaluate the effect of compound **18d** on the tumor cell cycle, we used flow cytometry to assay the PI-stained cells to determine the cell ratio in different cycles. As shown in Fig. 7, after **18d** treatment, H2228 cells in G0–G1 increased, while the number of cells in the S and G2–M phases decreased. Thus, it can be inferred that **18d** can prevent the cycle changes of tumor cells, making them stay in G0–G1 and unable to enter the late stage of division.

***In vivo* anti-tumor evaluation of compounds 18a–d in nude mice.**[8,30,31] *In vivo*, anti-tumor experiments are the most effective tools for evaluating active compounds before clinical study. Considering the species differences between humans and mice, we chose human-derived H2228 cells to form a xenograft model in nude mice. After subcutaneous injection of the H2228 cell suspension into the right armpits of nude mice for 10 days, the cells formed tumors. When the tumor volume reached about 200 m^3, compounds **18a–d** and the reference drug ceritinib were administered continuously at a dose of 20 mg kg^{-1} for 14 days, and the control group was administered an aqueous solution of

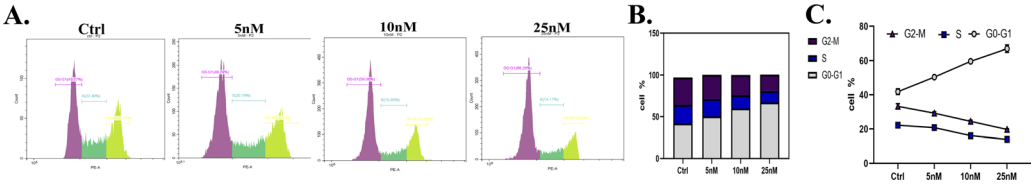

Fig. 7 (A) The cell cycle of H2228 cells after treatment with different doses of **18d**. (B) The ratio of each cell stage in the whole cell cycle. (C) The ratio changes at each stage after the intervention with different concentrations of **18d**.

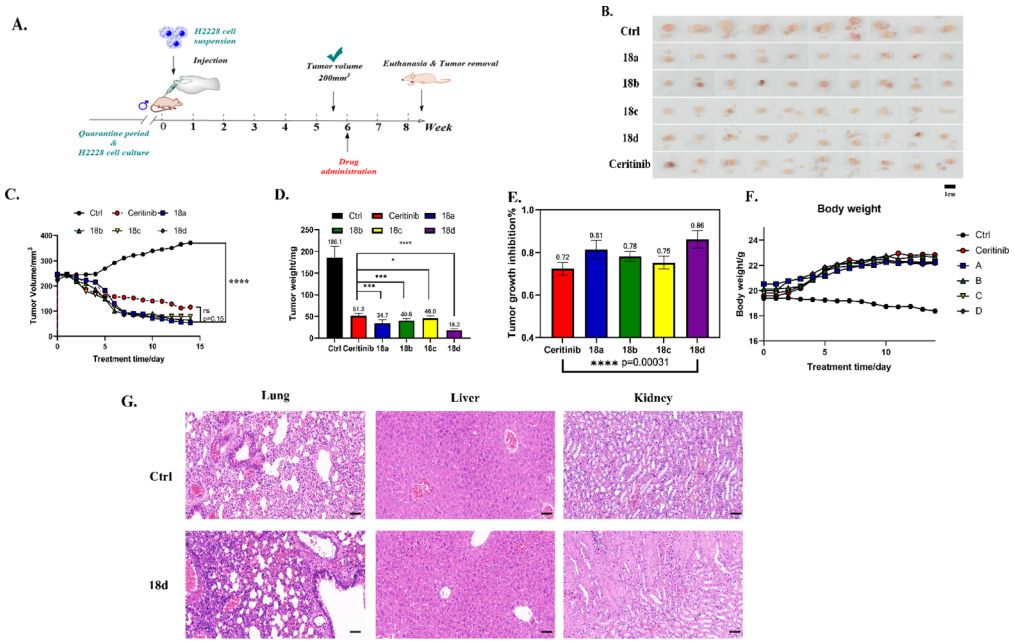

Fig. 8 (A) Experimental procedures and time points. (B) Images of tumors in each group. The scale bar is 1 cm. (C) The changes in the tumor volumes of nude mice in each group. The data were analyzed by the unpaired *t*-test (GraphPad Prism 8), and there were significant differences between the control group and **18a–d**, $P < 0.0001$. (D) The weights of tumors in each group. (E) Growth inhibition rate (TGI) of tumors in each group. (F) The body weight of each group after treatment. (G) Control and **18d** H&E staining results for the kidney, liver, and lung. The scale bar is 50 μm. The data are shown as the mean ± SD, and the unpaired two-way *t*-test (assuming all data with the same scatter) was used to determine the levels of significance between comparison samples. $p > 0.05$ was not significant (ns). *$p < 0.05$; **$p < 0.01$; ***$p < 0.001$; ****$p < 0.0001$.

CMC-Na. The volumes of tumors and weight changes in the nude mice were recorded every day. After the administration, the nude mice were euthanized and the tumors were removed carefully, then weighed and photographed. During the whole drug administration period, no death or abnormal behavior was observed and the weights of the **18a–d** group gradually increased, and so did those of the ceritinib group, which reflected that **18a–d** did not exhibit an obvious poisoning effect in nude mice at the dose of 20 mg kg^{-1}. We randomly chose one mouse in the control and **18d** group, took the liver, lung, and kidney for fixing, slicing, and H&E staining, and found that the slices of **18d** displayed no abnormal phenomena as compared with the control groups, which also proved the low toxicity of **18d**. The tumor volumes and tumor weights of the **18a–d** groups all decreased and were similar to, or better than, the ceritinib group. The TGI of **18d** is 86.3%, which is superior to that of the ceritinib group (72.8%). For the tumor volume changes, **18a** and **18d** displayed promising inhibitory effects of 191.63 and 184.89 mm^3, respectively, which are much higher as compared to the ceritinib group (131.00 mm^3) (Fig. 8).

Toxicity assay of compound 18d on human normal cells. In addition to the effectiveness of drugs, safety is also one of the important indicators for evaluating candidate drugs. For this purpose, we selected three different sources of normal cells (endothelial cells, liver cells, and kidney cells) for toxicity evaluation of **18d** toward human normal cells. The results in Table 2 indicate that **18d** has lower toxicity toward the three normal cells as compared to the positive drug ceritinib. For HK-2 and EA.hy926 cells, in particular, after incubation with ceritinib for 48 h, they displayed abnormal morphology changes, such as cell shrinkage or the formation of polygon-shaped cells (Fig. 9) (Table 3).

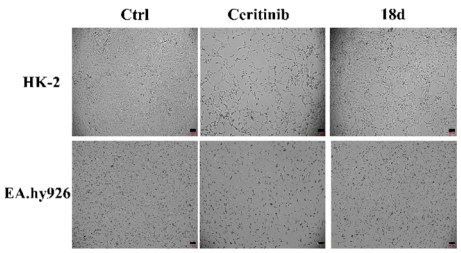

Fig. 9 HK-2 and EA.hy926 cell morphology when cultured with ceritinib or **18d** (both 1 μM), the scale bar is 100 μm.

Table 3 The results of the toxicity assay of compound **18d** on normal cells[a]

Compound **18a** IC_{50} μM		Ceritinib IC_{50} μM	
EA.hy926 (quiescent)	6.47 ± 0.95	EA.hy926 (quiescent)	2.44 ± 0.34
EA.hy926[b] (active)	8.92 ± 1.89	EA.hy926 (active)	3.42 ± 0.56
HK-2	5.79 ± 0.72	HK-2	1.44 ± 0.25
L02	>10	L02	3.42 ± 0.56

[a] The test results were obtained from at least three independent experiments. [b] EA.hy926 are activated by 10 mg mL^{-1} VEGF-containing medium.

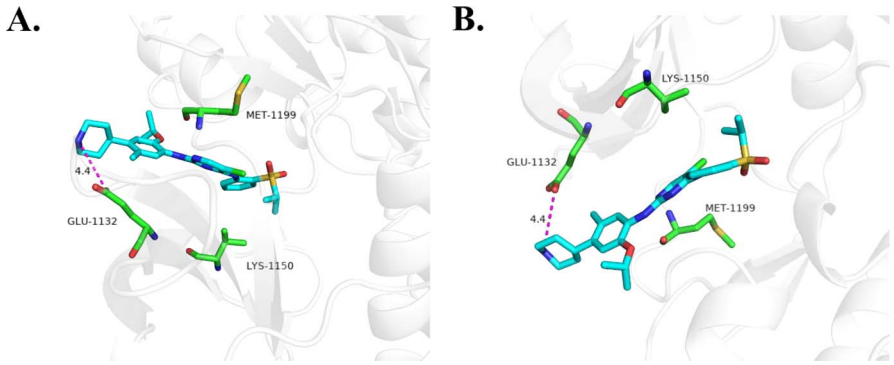

Fig. 10 (A) Molecular docking of **18d** with ALK kinase. (B) Molecular docking of ceritinib with ALK kinase.

Molecular docking study. To study the possible interactions of **18d** with ALK, we used Schrodinger Suites 2018 software to dock the compound with the active site of the kinase (PDB code: 2XB7). As shown in Fig. 10, **18d** and ceritinib are both located near the hinge region of the kinase. Hydrogen bonds are formed between the main chain nitrogen and oxygen of Met1199 through pyrimidine and amino nitrogen atoms of **18d**, respectively. The piperidine ring of **18d** extends into the solvent to form a salt bridge with Glu1210, and the sulfoxide group forms a hydrogen bond with Lys1150. These interactions are conducive to matching with the ALK active site (as shown in Fig. 10A). Compared with the positive drug ceritinib (as shown in Fig. 10B), the increased interaction between **18d** and ALK enhances the matching with the active site of ALK.

Conclusion

To develop new anti-cancer compounds with better activity and fewer side effects, we took the second-generation ALK inhibitor ceritinib as the lead and adopted strategies such as structural transformation and configuration control to synthesize a series of compounds with the pyrimidine core and sulfoxide group. Using CCK8 and MTT methods, Ba/F3-ALK, and the human non-small cell lung cancer cell line NCI-H2228, the anti-proliferative activity of the synthesized compounds was assayed with ceritinib as the reference. The results showed that most compounds exhibited good anti-tumor activity, and among them, **18a–d** showed slightly better activity than the reference. We conducted anti-tumor experiments on compounds **18a–d** in H2228 cell-modeled nude mice, and the results showed that the *in vivo* activities of all four compounds were superior to those of positive drugs. We also conducted the assay of the optimal compounds on human normal cell activity, and the results showed that the optimal compounds had lower IC_{50} values of anti-proliferative activity compared to the reference. The mechanism study showed that **18d** could result in cell apoptosis through the mitochondrial pathway. Moreover, **18d** also arrested the cancer cell cycle in the G0-G1 phase. In the cell signal pathway, **18d** could reduce the content of activated p-ALK, and p-STAT-3, without affecting ALK and STAT-3. In addition, preliminary studies on the toxicity of compound **18d** revealed that its toxicity toward several normal human cells was lower than that of the positive drug ceritinib. All these results indicate that compounds **18a–d** are good anti-tumor lead compounds and are worthy of further study.

Statistical analysis

All images were quantified by image *J* and the data analysis was conducted using GraphPad Prism 8. All experiments were repeated three times independently unless specifically indicated. The data are shown as the mean ± SD, and the unpaired two-way *t*-test (assuming all data with the same scatter) was used to determine the levels of significance between comparison samples. $p > 0.05$ was not significant (ns). $^{*}p < 0.05$; $^{**}p < 0.01$; $^{***}p < 0.001$; $^{****}p < 0.0001$.

Animal ethics

All experiments were carried out in accordance with the ethical requirements of laboratory animals. Laboratory animal use license number: SYXK (Guangdong) 2020-0102. Animal test certificate number: 00279323. After the end of the experiment, the animal carcasses were treated uniformly and harmlessly.

Author contributions

Han Yao is responsible for biology evaluation and animal experiment. Yuanyuan Ren is responsible for compound synthesis. Feng Wu carrys on structural characterization and elucidation of compounds. Jiadai Liu undertakes the docking part. Longcai Cao undertakes statistical analysis. Ming Yan provides financial support and overall planning. Xingshu Li propses the design and idea of the whole study.

Conflicts of interest

There are no conflicts to declare.

Acknowledgements

This research was funded by National Natural Science Foundation of China, grant number 82061128001.

References

1 J. J. Lin, G. J. Riely and A. T. Shaw, Targeting ALK: Precision Medicine Takes on Drug Resistance, *Cancer Discovery*, 2017, **7**(2), 137–155.
2 T. Li, S. E. Stayrook, Y. Tsutsui, *et al.*, Structural basis for ligand reception by anaplastic lymphoma kinase, *Nature*, 2021, **600**(7887), 148–152.
3 A. V. Reshetnyak, P. Rossi, A. G. Myasnikov, *et al.*, Mechanism for the activation of the anaplastic lymphoma kinase receptor, *Nature*, 2021, **600**(7887), 153–157.
4 N. Haratake, G. Toyokawa, T. Seto, *et al.*, The mechanisms of resistance to second- and third-generation ALK inhibitors and strategies to overcome such resistance, *Expert Rev. Anticancer Ther.*, 2021, **21**(9), 975–988.
5 S. M. Barrows, K. Wright, C. Copley-Merriman, *et al.*, Systematic review of sequencing of ALK inhibitors in ALK-positive non-small-cell lung cancer, *Lung Cancer*, 2019, **10**, 11–20.
6 X. Du, Y. Shao, H. F. Qin, *et al.*, ALK-rearrangement in non-small-cell lung cancer (NSCLC), *Thorac. Cancer*, 2018, **9**(4), 423–430.
7 R. Chiarle, C. Martinengo, C. Mastini, *et al.*, The anaplastic lymphoma kinase is an effective oncoantigen for lymphoma vaccination, *Nat. Med.*, 2008, **14**(6), 676–680.
8 T. H. Marsilje, W. Pei, B. Chen, *et al.*, Synthesis, structure–activity relationships, and *in vivo* efficacy of the novel potent and selective anaplastic lymphoma kinase (ALK) inhibitor 5-chloro-*N*2-(2-isopropoxy-5-methyl-4-(piperidin-4-yl)phenyl)-*N*4-(2-(isopropylsulfonyl)phenyl)pyrimidine-2,4-diamine (LDK378) currently in phase 1 and phase 2 clinical trials, *J. Med. Chem.*, 2013, **56**(14), 5675–5690.
9 S. Peters, D. R. Camidge, A. T. Shaw, *et al.*, Alectinib *versus* Crizotinib in Untreated ALK-Positive Non-Small-Cell Lung Cancer, *N. Engl. J. Med.*, 2017, **377**(9), 829–838.
10 D. R. Camidge, H. R. Kim, M. J. Ahn, *et al.*, Brigatinib *versus* Crizotinib in Advanced ALK Inhibitor-Naive ALK-Positive Non-Small Cell Lung Cancer: Second Interim Analysis of the Phase III ALTA-1L Trial, *J. Clin. Oncol.*, 2020, **38**(31), 3592–3603.
11 R. Bentley, Role of sulfur chirality in the chemical processes of biology, *Chem. Soc. Rev.*, 2005, **34**(7), 609–624.
12 W. R. F. Goundry, B. Adams, H. Benson, *et al.*, Development and Scale-up of a Biocatalytic Process To Form a Chiral Sulfoxide, *Org. Process Res. Dev.*, 2017, **21**(1), 107–113.
13 T. Matsui, Y. Dekishima and M. Ueda, Biotechnological production of chiral organic sulfoxides: current state and perspectives, *Appl. Microbiol. Biotechnol.*, 2014, **98**(18), 7699–7706.
14 H. J. Federsel, Facing chirality in the 21st century: approaching the challenges in the pharmaceutical industry, *Chirality*, 2003, **15**, S128–S142.
15 K. Okamoto and T. Nishino, Mechanism of inhibition of xanthine oxidase with a new tight binding inhibitor, *J. Biol. Chem.*, 1995, **270**(14), 7816–7821.
16 M. Matsugi, R. Shimada, S. Ohata, *et al.*, The improved synthesis of OPC-29030, a platelet adhesion inhibitor *via* diastereoselective oxidation of chiral non-racemic sulfide, *Chem. Pharm. Bull.*, 2002, **50**(11), 1511–1513.
17 Y. Ozeki, Y. Nagamura, H. Ito, *et al.*, An anti-platelet agent, OPC-29030, inhibits translocation of 12-lipoxygenase and 12-hydroxyeicosatetraenoic acid production in human platelets, *Br. J. Pharmacol.*, 1999, **128**(8), 1699–1704.
18 C. L. Defty and J. R. Marsden, Melphalan in regional chemotherapy for locally recurrent metastatic melanoma, *Curr. Top. Med. Chem.*, 2012, **12**(1), 53–60.
19 AstraZeneca UK Limited and AstraZeneca AB. Swed, *Morpholinio Pyrimidines and Their Use in Therapy*, WO2011154737A1, 2011.
20 A. T. Shaw, T. M. Bauer, F. De Marinis, *et al.*, First-Line Lorlatinib or Crizotinib in Advanced ALK-Positive Lung Cancer, *N. Engl. J. Med.*, 2020, **383**(21), 2018–2029.
21 K. Iikubo, Y. Kondoh, I. Shimada, *et al.*, Discovery of *N*-{2-Methoxy-4-[4-(4-methylpiperazin-1-yl)piperidin-1-yl]phenyl}-*N*′-[2-(propane-2-sulfonyl)phenyl]-1,3,5-triazine-2,4-diamine (ASP3026), a Potent and Selective Anaplastic Lymphoma Kinase (ALK) Inhibitor, *Chem. Pharm. Bull.*, 2018, **66**(3), 251–262.
22 J. Wang, M. Sánchez-Roselló, J. L. Aceña, *et al.*, Fluorine in pharmaceutical industry: fluorine-containing drugs introduced to the market in the last decade (2001–2011), *Chem. Rev.*, 2014, **114**(4), 2432–2506.
23 S. Purser, P. R. Moore, S. Swallow, *et al.*, Fluorine in medicinal chemistry, *Chem. Soc. Rev.*, 2008, **37**(2), 320–330.
24 R. Peters, Carbon-fluorine compounds: chemistry, biochemistry and biological activities, *Ciba Found. Symp.*, 1971, **2**, 1–7.
25 X. Zhang, T. Yang, X. Jin, K. Lin, X. Dai, T. Gao, G. Huang, M. Fan, L. Ma, Z. Liu and J. Cao, Synthesis and biological evaluation of cytotoxic activity of novel podophyllotoxin derivatives incorporating piperazinyl-cinnamic amide moieties, *Bioorg. Chem.*, 2022, **123**, 105761, DOI: **10.1016/j.bioorg.2022.105761**.
26 Q. Dou, H. N. Chen, K. Wang, K. Yuan, Y. Lei, K. Li, J. Lan, Y. Chen, Z. Huang, N. Xie, L. Zhang, R. Xiang, E. C. Nice, Y. Wei and C. Huang, Ivermectin Induces Cytostatic Autophagy by Blocking the PAK1/Akt Axis in Breast Cancer, *Cancer Res.*, 2016, **76**(15), 4457–4469, DOI: **10.1158/0008-5472.CAN-15-2887**.
27 X. Wang, X. Lu, R. Zhu, et al., Betulinic Acid Induces Apoptosis in Differentiated PC12 Cells *via* ROS-Mediated Mitochondrial Pathway, *Neurochem Res*, 2017, **42**, 1130–1140, DOI: **10.1007/s11064-016-2147**; J. Lopez and S. W. Tait, Mitochondrial apoptosis: killing cancer using the enemy within, *Br. J. Cancer*, 2015, **112**(6), 957–962, DOI: **10.1038/bjc.2015.85**.
28 Y. Lu, Z. Fan, S. J. Zhu, *et al.*, A new ALK inhibitor overcomes resistance to first- and second-generation inhibitors in NSCLC, *EMBO Mol. Med.*, 2022, **14**(1), e14296, DOI: **10.15252/emmm.202114296**.
29 T. Pan, Y. Dan, D. Guo, *et al.*, Discovery of 2,4-pyrimidinediamine derivatives as potent dual inhibitors of

ALK and HDAC, *Eur. J. Med. Chem.*, 2021, **224**, 113672, DOI: 10.1016/j.ejmech.2021.113672.

30 E. F. Mesaros, T. V. Thieu, G. J. Wells, *et al.*, Strategies to mitigate the bioactivation of 2-anilino-7-aryl-pyrrolo[2,1-f][1,2,4]triazines: identification of orally bioavailable, efficacious ALK inhibitors, *J. Med. Chem.*, 2012, **55**(1), 115–125, DOI: 10.1021/jm2010767.

31 We encourage the citation of primary research over review articles, where appropriate, in order to give credit to those who first reported a finding. Find out more about our commitments to the principles of San Francisco Declaration on Research Assessment (DORA).